

Parameter Range of ICRF Heated Plasma on Large Helical Device

R.Kumazawa, T.Mutoh, T.Seki, K.Saito, T.Watari, M.Osakabe, S.Murakami, M.Sasao, T.Watanabe, T.Yamamoto¹, Y.Torii¹, T.Notake¹, N.Takeuchi¹, H.Matshita¹, T.Saida², F.Shimpo, G.Nomura, M.Yokota, Zhao Yanping³, H.Okada⁴, M.Isobe, T.Ozaki, K.Narihara, Y.Nagayama, S.Inagaki, S.Morita, A.V.Krasilnikov⁵, H.Idei, S.Kubo, K.Ohkubo, M.Sato, T.Shimozuma, Y.Yoshimura, K.Ikeda, Y.Oka, Y.Takeiri, K.Tsumori, K.Nagaoka, N.Ashikawa, M.Emoto, H.Funaba, M.Goto, K.Ida, T.Kobuchi, Y.Liang³, S.Masuzaki, T.Minami, J.Miyazawa, T.Morisaki, S.Muto, Y.Nakamura, H.Nakanishi Y.Narushima, K.Nishimura, N.Noda, S.Ohdachi, B.J.Peterson, A.Sagara S.Sakakibara, R.Sakamoto, K.Sato, M.Shoji, H.Suzuki, K.Tanaka, K.Toi, T.Tokuzawa, K.Y.Watanabe, I.Yamada, Y.Yoshinuma, K.Yamazaki, M.Yokoyama, K-Y.Watanabe, O.Kaneko, K.Kawahata, A.Komori, N.Ohyabu, H.Yamada, S.Sudo, Y.Hamada, O.Motojima, M.Fujiwara and LHD Experimental Group

National Institute for Fusion Science, Toki 509-5292, Japan

¹*Nagoya University, Nagoya 464-8601, Japan*

²*The Graduate University for Advanced Studies, Toki, Japan*

³*Institute of Plasma Physics Academia Sinica, Hefei 230031, P.R.China*

⁴*Kyoto University, Uji, Kyoto 611-0011, Japan*

⁵*Troitsk Institute for Innovating and Fusion Research (TRINITI), Troitsk, Russia*

A difference in the confinement performance of high energy ions between the standard and the inward-shifted magnetic axis configurations on the Large Helical Device was experimentally observed in the ion cyclotron range of frequency (ICRF) heated plasma. It caused a difference in the transfer efficiency from high energy ions to a bulk plasma, which was compared with the Monte Carlo simulation result. The ratio of the stored energy of the high energy ions to that of the bulk plasma was measured employing an ICRF heating power modulation method.

1. Introduction

The ion cyclotron range of frequency (ICRF) heating has been successfully carried out on the Large Helical Device (LHD, the largest superconducting helical device, with $R/a=3.6\sim 3.9\text{m}/0.6\text{m}$, $B=3\text{T}$) [1-3]. A long pulse discharge of 2 minutes was achieved by ICRF heating only. The energy confinement time was found to be 1.5 times longer than International Stellarator Scaling 95 (ISS95) at the inward-shifted magnetic axis, i.e., $R_{ax}=3.6\text{m}$. This was derived from the fact that the displacement of deeply trapped particles in the helical ripple from the magnetic closed surface was reduced at $R_{ax}=3.6\text{m}$. The phenomenon is thought to be similar to that of the high energy ions accelerated by an RF electric field; the confinement of high energy ions is better and the energy transfer efficiency is expected to be higher than that at the standard configuration, i.e., $R_{ax}=3.75\text{m}$. The difference between the magnetic configurations was examined measuring the energy distribution of high energy ions.

The technique of RF power modulation was used to evaluate energy confinement time and

heating efficiency [4]. This method was employed to deduce the ratio of the stored energy of high energy ions to the bulk plasma. It was determined from two phase differences; one was between the total plasma stored energy and the bulk plasma stored energy, and the other was a phase difference between the modulated RF power and the total plasma stored energy.

In this paper the confinement of high energy ions is discussed using experimental data obtained in a series of plasma discharges at the standard ($R_{ax}=3.75m$) and the inward-shifted ($R_{ax}=3.6m$) magnetic configurations. Then it is compared with the result obtained in the Monte Carlo simulation [5]. Then the measured ratio of the stored energy was reported for the plasma discharge with an ICRF power modulation method.

2. Experimental results

Tail temperature and transfer efficiency

A plasma consisting of He ions as the majority and H ions as the minority was employed in the series of experiments. The relation between tail temperature T_{tail} and effective temperature T_{eff} is plotted in Fig.1. T_{tail} was measured using a fast-neutral analyzer (Si-FNA) with an electrically cooled Silicon-diode detector [6] and the charge exchange process with 4He [7]. The Si-FNA measured ions with the perpendicular energy to the magnetic field line. T_{eff} was calculated using plasma parameters (n_H , n_e and T_e are the minority ion density, the electron density and the temperature) and the ICRF heating power P_A in the following equation [8];

$$T_{eff} \approx A \frac{\eta_H (n_H/n_e) P_A T_e^{3/2}}{(n_H/n_e) n_e^2 V_H}, \quad T_{tail} \approx \frac{\tau_E^{tail}}{\tau_s/2} T_{eff}, \quad \frac{1}{\tau_E^{tail}} = \frac{1}{\tau_s/2} + \frac{1}{\tau_E^{loss}}$$

Here η_H and V_H are the heating efficiency and the minority heating volume [9]. A wide range of T_{eff} to be precise from 10keV to 200keV was found at $R_{ax}=3.75m$; however the range of T_{eff} at $R_{ax}=3.6m$ was from 10 to 60keV, which was caused by an insufficient reduction of the minority ion density. A saturation of T_{tail} was found at $R_{ax}=3.75m$; this reflects a shorter energy loss time. When the energy loss time τ_E^{loss} was taken into account and the tail energy time τ_E^{tail} was

determined, T_{tail} was calculated using the above equation.

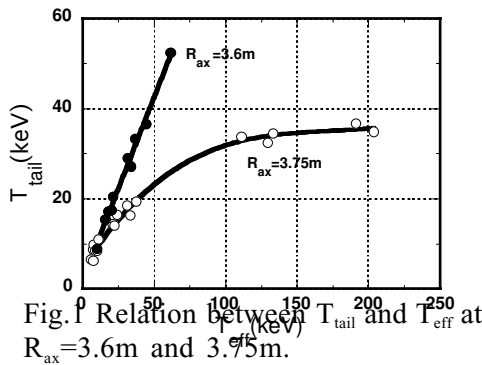


Fig.1 Relation between T_{tail} and T_{eff} at $R_{ax}=3.6m$ and $3.75m$.

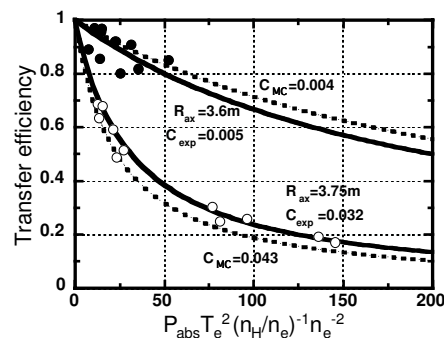


Fig.2 Dependence of transfer efficiency on $P_{abs} T_e^2 (n_H/n_e)^{-1} n_e^{-2}$ at $R_{ax}=3.6m$ and $3.75m$.

The transfer efficiency η_{trms} was defined as what fraction of the energy flows from high energy ions to the bulk plasma;

$$\eta_{trms} = \frac{P_{trms}}{P_{abs}} = \frac{T_{tail}}{T_{eff}} = \frac{1}{1 + CP_{abs} T_e^2 (n_H/n_e)^{-1} n_e^{-2}}$$

It was also expressed as the ratio of T_{tail} to T_{eff} . In the Monte Carlo simulation η_{trms} was scaled as in the above equation. Here the numerical factor C depends on the magnetic axis position and the magnetic strength. It was determined using experimental data for two cases as shown in Fig.2, where the abscissa is $P_{abs} T_e^2 (n_H/n_e)^{-1} n_e^{-2}$. C_{exp} was determined to be 0.032 at $R_{ax}=3.75m$ and 0.005 at $R_{ax}=3.6m$, respectively. C_{MC} in the Monte Carlo simulation was also 0.043 at $R_{ax}=3.75m$ and 0.004 at $R_{ax}=3.60m$ [5].

High energy tail fraction

An analysis of the plasma discharge with the RF power modulation predicts a ratio of the stored energy of high energy ions to that of the bulk plasma using two phase differences. One was between the bulk plasma W_b and the total plasma stored energy W_p including the store energy of high energy ions, and the other was between the modulated RF power P_A and W_p . The relations between δW_p and δW_b , and between δP_A and δW_p are expressed in the following complex equation [4],

$$\begin{aligned} \frac{\delta W_p}{\delta W_b} &= 1 + \frac{3}{2} \frac{AR_{tb}}{\eta_{trms}} + i \frac{3}{2} \omega \tau_{se0} / 2 \\ \frac{\delta W_p}{\delta P_A} &= \eta_{trms} \tau_{se0} / 2 \eta_0 \frac{1 + \frac{3}{2} (i\omega \tau_{se0} / 2 + \frac{AR_{tb}}{\eta_{trms}})}{-BR_{tb} + (i\omega \eta_{trms} \tau_{se0} / 2 + 1)(i\omega \tau_{se0} / 2 + \frac{AR_{tb}}{\eta_{trms}})} \\ A &= \frac{3}{2} + (1 - \beta), \quad B = \frac{\eta' T_0}{\eta_0} + \frac{3}{2} \end{aligned}$$

ω and β are the applied modulation frequency and a numerical factor derived from the dependence of the energy confinement time on the temperature; $\beta = -1.44$ at ISS95. η_0 is the heating efficiency and η' is its derivative of temperature [4]. The phase difference between δW_p and the bulk plasma was θ_{pb} and the phase difference between δP_A and δW_p was θ_{pA} ; δW_p was used as the diamagnetic loop and δW_b was used as ECE signal because of no observed modulated electron density. The time evolutions of P_A , W_p and W_b in the case of the low electron density plasma with $n_e = 2 \sim 3 \times 10^{18} m^{-3}$ are shown in Fig.3(a). The averaged RF power was $P_A = 270kW$ and the modulation rate was 30%. θ_{pb} and θ_{pA} were 20 degrees and -56 degrees at $t=1.0s$ and $n_e = 2.2 \times 10^{18} m^{-3}$, and at $t=2.0s$ and the higher electron density, i.e., $n_e = 3 \times 10^{18} m^{-3}$, θ_{pb} and θ_{pA} were 11 degrees and -36 degrees as shown in Fig.3(b). The measured ratio of W_t to W_b was deduced to be $R_{tb} = 0.4 \sim 0.2$ using measured phases in the above equation. This value was assessed in another way by using the electron slowing down time $\tau_s/2$ and half of the

ISS95 confinement time at the collisionless regime in $R_{ax}=3.75m$ [10]. The ratio of $\tau_s/2/\tau_{E0}/2$ was calculated to be 0.4~0.2.

3. Summary

The ICRF heating experiments on the LHD was carried out successfully. The confinement characteristics of high energy ions accelerated by ICRF electric field were examined measuring the energy distribution with the Si-diode detector. As predicted in the orbit calculation, the better confinement of the high energy ions at the inward-shifted configuration compared with that at the standard configuration was proved. These experimental data agree with the transfer efficiency obtained in the Monte Carlo simulation.

The ratio of the stored energy of the high energy component W_i to that of the bulk plasma W_b was measured in the ICRF power modulated plasma. The ratio agreed with that deduced from the ratio of the electron slowing down time to the energy confinement time.

Acknowledgement

The authors thank the scientists and the technical staff who operated the LHD at the National Institute for Fusion Science.

References

- [1] Mutoh T et al Phys. Rev. Lett. **85** 4530
- [2] Watari T et al Nucl. Fusion **41** 325
- [3] Kumazawa R et al Phys. Plasmas **8** 2139
- [4] Torii Y et al Plasma Phys. Controlled Fusion **43** 1191
- [5] Murakami S et al Nucl. Fusion **39** 1165
- [6] Osakabe M et al Rev. of Scientific Inst. **72** 590 & 788
- [7] Krashilnikov et al Nucl. Fusion **42** 759
- [8] Stix T H Nuclear Fusion **15**(1975) 737
- [9] Saito K et al Nucl. Fusion **41** 1021
- [10] Yamada H et al Plasma Phys. Controlled Fusion **43** A55

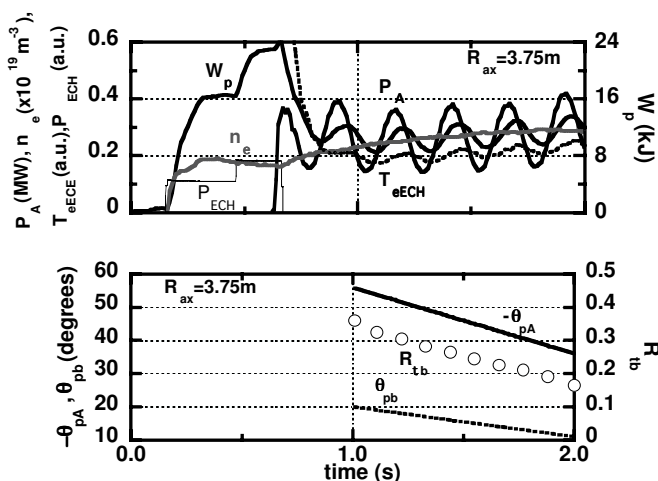


Fig.3(a) Time evolutions of P_A, W_p and T_{eECE} at $R_{ax}=3.75m$.

(b) Time evolutions of measured phase difference θ_{pA} and θ_{pB} and R_{ib} .